ImmunoTargets and Therapy

Dovepress
Taylor & Francis Group

Open Access Full Text Article

ORIGINAL RESEARCH

Anlotinib Combined with Programmed Death-1/Programmed Death-Ligand 1 Inhibitor 9 Hydrochloride Suppresses Colorectal Cancer Progression by Inducing Neovascularization and Reprogramming the Tumor Immune Microenvironment in MSS Murine Model

Junpeng Ma[1–4,*], Mingkun Wang[4,5,*], Kunnan Wang[4,5,*], Juyi Wen[6], Xiaoya Liu[5], Xiangfei Zhao[4,6]

[1]Department of Hepatobiliary and Pancreatic Surgery, Beijing Tsinghua Changgung Hospital, School of Clinical Medicine, Tsinghua Medicine, Tsinghua University, Beijing, People's Republic of China; [2]Department of Hepatobiliary Intervention, Beijing Tsinghua Changgung Hospital, School of Clinical Medicine, Tsinghua Medicine, Tsinghua University, Beijing, People's Republic of China; [3]Yttrium-90 Precision Interventional Radiotherapy Center, School of Clinical Medicine, Tsinghua Medicine, Tsinghua Changgung Hospital, Tsinghua University, Beijing, People's Republic of China; [4]Navy Clinical College, the Fifth School of Clinical Medicine, Anhui Medical University, Hefei, Anhui, People's Republic of China; [5]Department of General Surgery, The Sixth Medical Center of Chinese PLA General Hospital, Beijing, People's Republic of China; [6]Senior Department of Oncology, Chinese PLA General Hospital, Beijing, People's Republic of China

*These authors contributed equally to this work

Correspondence: Xiangfei Zhao, Senior Department of Oncology, Chinese PLA General Hospital, Beijing, People's Republic of China, Email article1977@163.com

ImmunoTargets and Therapy downloaded from https://www.dovepress.com/
For personal use only.

Background: Anlotinib, a novel multi-target tyrosine kinase inhibitor, has demonstrated promising antitumor efficacy by inhibiting angiogenesis. However, the potential therapeutic benefits and underlying mechanisms of combining anlotinib with immune checkpoint inhibitors in colorectal cancer remain unclear.

Methods: Syngeneic models of colorectal cancer were established and treated with anlotinib, PD-1/PD-L1-IN-9 hydrochloride, or their combination. Tumor tissues were analyzed using immunohistochemistry, and Western blotting to assess angiogenesis-associated markers, tissue hypoxia, and key molecular markers. Flow cytometry, ELISA, and immunostaining were performed to evaluate immune cell infiltration, cytokine expression, and the tumor immune microenvironment.

Results: The combination of anlotinib and PD-1/PD-L1-IN-9 hydrochloride significantly inhibited tumor growth compared to monotherapy, associated with improved neovascularization and alleviated hypoxia. Combined therapy increased CD8+ T cell infiltration, reduced immunosuppressive cell populations, and partially modulated cytokine profiles, thereby enhancing the antitumor immune response.

Conclusion: Anlotinib combined with PD-1/PD-L1-IN-9 hydrochloride exhibits superior antitumor efficacy in colorectal cancer compared to either agent alone, potentially by reshaping the tumor microenvironment. These findings support further exploration of combined anti-angiogenic and immune checkpoint therapy as a promising strategy for colorectal cancer treatment.

Keywords: anlotinib, PD-1/PD-L1-IN-9 hydrochloride, colorectal cancer, tumor immune microenvironment, MSS Murine Model

Introduction

Colorectal cancer (CRC) is a common malignancy of the gastrointestinal tract, with a high incidence and mortality rate worldwide.[1] Despite significant advances in early screening and adjuvant therapies, the 5-year survival rate for patients diagnosed with advanced metastatic colorectal cancer remains only 10%.[2] Although surgical, chemotherapeutic,

https://doi.org/10.2147/ITT.S597338
Received: 20 January 2026
Accepted: 27 May 2026
Published: 30 June 2026

© 2026 Ma et al. This work is published and licensed by Dove Medical Press Limited. The full terms of this license are available at https://www.dovepress.com/terms.php and incorporate the Creative Commons Attribution – Non Commercial (unported, v4.0) License (http://creativecommons.org/licenses/by-nc/4.0/). By accessing the work you hereby accept the Terms. Non-commercial uses of the work are permitted without any further permission from Dove Medical Press Limited, provided the work is properly attributed. For permission for commercial use of this work, please see paragraphs 4.2 and 5 of our Terms (https://www.dovepress.com/terms.php).

radiotherapeutic, and molecular-targeted treatments have improved survival, the prognosis of metastatic CRC remains poor, and palliative chemotherapy is still the mainstay treatment.[3]

With the approval of drugs such as inhibitors of programmed cell death receptor 1 (PD-1), programmed cell death ligand 1 (PD-L1), and cytotoxic T-lymphocyte-associated protein 4 (CTLA-4), immune checkpoint inhibitors (ICI) has become a hot topic in cancer research and has shown success in several malignancies.[4] However, most CRC patients do not benefit, and clinical responses are largely restricted to the small subset with mismatch repair deficiency/microsatellite instability-high (dMMR/MSI-H) tumors. In contrast, the vast majority of CRC patients have microsatellite-stable (MSS) tumors, which generally respond poorly to immune checkpoint blockade.[5,6] Thus, expanding the proportion of CRC patients who benefit from immunotherapy is an urgent issue to be addressed. Overcoming immunotherapy resistance in MSS CRC represents a critical clinical dilemma.

The tumor microenvironment (TME), composed of blood vessels, stromal cells, and immune cells, is characterized by abnormal vasculature, hypoxia, and immunosuppression, which significantly reduces the effectiveness of cancer treatment including immunotherapy.[7,8] In particular, abnormal tumor vasculature not only impairs drug and immune cell delivery but also exacerbates hypoxia, which in turn promotes the recruitment of immunosuppressive cells and induces resistance to immune checkpoint blockade. These interconnected features of the TME are critically involved in the poor response of MSS CRC to immunotherapy. Therefore, strategies that normalize the TME may improve therapeutic efficacy.

Tumor angiogenesis is a key process in cancer development and metastasis, with vascular endothelial growth factor (VEGF) and its receptor VEGFR2 playing significant roles and being associated with cancer immune evasion.[9] Anti-angiogenic therapy can normalize abnormal tumor vessels, improve oxygenation, and enhance immune cell infiltration, thereby potentially synergizing with immunotherapy.[10,11] Anlotinib, a multi-target tyrosine kinase inhibitor of VEGFR, FGFR, PDGFR, and c-kit, has been approved in China for the treatment of several solid tumors.[12] However, anlotinib monotherapy has shown limited efficacy in controlling tumor progression, which may be attributed to its inability to durably reverse the immunosuppressive TME or fully overcome vascular abnormalities and hypoxia. Preclinical studies have shown that combining anti-angiogenic therapy with PD-1/PD-L1 blockade can improve T-cell infiltration and antitumor efficacy in various cancers,[13,14] and anlotinib has also been reported to transiently normalize vasculature and augment PD-1 blockade.[15] Nevertheless, whether anlotinib combined with PD-1 inhibition can effectively reverse the vascular, hypoxic, and immunosuppressive features of the TME and thereby enhance antitumor immunity in MSS CRC remains unknown. In this study, we investigated the effects of this combination in a murine MSS CRC model, focusing on tumor growth, survival, vascular remodeling, and immune microenvironment reprogramming, to provide experimental evidence for new therapeutic strategies.

Materials and Methods

Cell Culture and Heterotopic Tumor Transplantation Model

The colorectal cancer cell line CT26 was acquired from the American Type Culture Collection (ATCC). CT26 is a widely used immunocompetent murine colorectal cancer model in BALB/c mice and allows evaluation of tumor–immune interactions in a syngeneic setting with an intact immune system. The cells were maintained in Dulbecco's Modified Eagle Medium (DMEM) supplemented with 10% fetal bovine serum (FBS) and antibiotics (100 μg/mL penicillin/streptomycin) and cultured at 37°C in a 5% CO_2 atmosphere. Cells were passaged upon reaching 80–90% confluence using 0.25% trypsin-EDTA. Cells in the exponential growth phase were used in subsequent experiments. For subcutaneous injection, CT26 cells were harvested, washed twice with sterile PBS, and resuspended in sterile PBS (pH 7.4) as the injection buffer. CT26 cells were injected subcutaneously into the right flank of BALB/c mice.

The animal use protocol listed below was reviewed and approved by the Animal Ethics Committee of Zhongyan Zichuang (Beijing) Biotechnology Co., Ltd. (Ethics number ZYZC202402011S). In this study, we purchased a total of 48 BALB/c mice (male, 18~20 g, 5 weeks old) from Spefor Biotechnology Co., Ltd. (Beijing, China). In particular, 24 mice for endpoint tumor harvesting and tissue analyses and 24 mice for survival analysis. All animals were acclimatized under specific pathogen-free conditions for 1 week, provided with sterilized food and water. The mice were randomly divided into four groups (n=6): a control group receiving vehicle treatment with PBS, an anlotinib-only treatment group, a PD-1/PD-L1-IN-9 hydrochloride-only treatment group, and a combination of anlotinib and PD-1/PD-L1-IN-9 hydrochloride

treatment group. A heterotopic colorectal cancer model was established by subcutaneous injection of 5 × 10^5 CT26 cells resuspended in 100 μL sterile PBS into the right flank of BALB/c mice on day 0. The control group (NC) received vehicle treatment with PBS under the same injection schedule as the treatment groups. The Anlotinib group received 3 mg/kg anlotinib (Chia Tai Tianqing Pharmaceutical Group Co., Ltd.) by gavage from day 1 to day 10 (d1-d10), the PD-1/PD-L1-IN-9 hydrochloride group received intraperitoneal injections of PD-1/PD-L1-IN-9 hydrochloride (PD-1/PD-L1-IN-9, HY-132192, Med Chem Express). The dosage of 10 mg/kg administered intraperitoneally every three days (d1, d4, d7, d10) was selected according to the manufacturer's recommendation and has been validated in previous preclinical studies.[16] The Combination group received daily gavage of 3 mg/kg anlotinib from day 1 to day 10 (d1-d10), and anti-PD-1 inhibitor treatment (intraperitoneal injection of 10 mg/kg PD-1/PD-L1-IN-9 hydrochloride) on days 1, 4, 7, and 10, identical to the monotherapy group. Tumor volume was measured on days 1, 4, 7, 11, and 15 (calculation formula: tumor volume = (length × width^2) /2). On day 15, mice were injected intraperitoneally with sodium pentobarbital solution (50 mg/kg, i.p),[17] following profound anesthesia, tumors were surgically excised, weighed, and appropriately preserved for further examination.

For flow cytometric analysis of tumor-infiltrating immune cells, fresh tumor tissues were finely minced and digested in RPMI 1640 medium containing 1 mg/mL collagenase IV and 0.1 mg/mL DNase I for 30 minutes at 37°C with gentle shaking. The digested tissue was then passed through a 70 μm cell strainer to obtain a single-cell suspension. After washing with PBS containing 2% FBS, red blood cells were lysed using ACK lysis buffer. Cells were washed twice and resuspended in staining buffer. Viable cells were counted using trypan blue exclusion. To exclude doublets and dead cells, single cells were gated by FSC-H vs FSC-A, and dead cells were excluded using Zombie NIR™ according to the manufacturer's instructions. Cells were then incubated with Fc block for 10 minutes, followed by surface antibody staining for 30 minutes at 4°C. After staining, cells were washed and fixed with 1% paraformaldehyde before acquisition on a flow cytometer. Data were analyzed using FlowJo software.

Survival Analysis

For survival analysis, 6 mice were randomly selected from each of the four experimental groups. The experiment commenced from the first day of medication, marked as day 1, and continued until a reasonable end to the experiment. For survival analysis, humane endpoints were defined as tumor volume ≥ 2000 mm^3or severe distress. Mice reaching these criteria were euthanized immediately.

Antibodies and Reagents

Antibodies used for Western blot and flow cytometry analyses are listed in Supplementary Table S1. Goat anti-rabbit secondary antibody was purchased from AFFINITY (1:10,000, S0001, Affinity Biosciences).

Flow Cytometry Analysis

Colorectal cancer cells were harvested and centrifuged at 400 × g (or 1,500 rpm) for 5 minutes. For cell surface staining, the resulting cell suspension was washed twice in PBS, stained with specified fluorescently-labeled antibodies on ice for 30 minutes, and then subjected to additional PBS washes. For intracellular staining, cells were fixed and permeabilized using the Cytofix/CytoPerm BUF KIT (BD Pharmingen, catalog number 554714). For analyzing tumor immune cell infiltration, a similar staining protocol was followed: at day 15, tumors were excised from mice, weighed, mechanically disrupted, and digested with collagenase IV (17104019, Thermo Fisher) to generate single-cell suspensions. All samples were analyzed by flow cytometry using either an LSRFortessa (BD Biosciences) or Navios and Gallios instruments (Beckman Coulter), with data processed using FlowJo software version 10.8.1 according to the manufacturer's instructions. After excluding doublets and dead cells, analyses focused on $CD45^+$ leukocytes, within which $CD4^+$ and $CD8^+$ T cells were identified as $CD45^+CD4^+$ and $CD45^+CD8^+$ subsets, respectively, regulatory T cells (Tregs) were defined as $CD45^+CD4^+CD25^+FOXP3^+$ cells, tumor-associated macrophages (TAMs) as $CD45^+CD11b^+F4/80^+CD163^+$ cells, and myeloid-derived suppressor cells (MDSCs) as $CD45^+CD11b^+Ly6C^+/Ly6G^+$ subsets.

Western Blot Analysis

Following different treatments, tumor tissues were collected and lysed in RIPA lysis buffer containing phosphatase and protease inhibitors (MedChemExpress, Monmouth Junction, NJ, USA) for total protein extraction. Protein concentration was determined using the BCA Protein Assay Kit (P0010, Beyotime, Shanghai, China) according to the manufacturer's instructions. Samples were boiled for 5 minutes in loading buffer. The lysates were separated by 10% SDS-PAGE and transferred onto polyvinylidene difluoride membranes (IPVH00010, Millipore, Burlington, MA, USA). Membranes were blocked with 5% bovine serum albumin at room temperature for 2 hours, then incubated with primary antibodies overnight at 4°C. After washing with TBST, membranes were incubated with secondary antibodies (1:10,000, S0001, Affinity Biosciences) at room temperature for 1 hour. Following another round of washing with TBST, protein bands were detected using ECL detection reagent (P0018S, Beyotime). Images were quantified using Image J software (National Institutes of Health, Bethesda, MD, USA) based on three independent biological replicates and normalized to GAPDH (Supplementary Figure S1–S7).

Immunohistochemistry Analysis

Tumor tissue samples fixed in 4% paraformaldehyde were embedded in 4% paraffin, and continuous sections (3 μm thick) were prepared. After deparaffinization and hydration, antigen retrieval was performed using 10 mM Citrate Buffer (pH 6.0). Sections were then incubated with 5% bovine serum albumin at room temperature for 45 minutes to block nonspecific binding sites. Apoptosis was detected using the TUNEL Assay Kit (Beyotime Biotech Inc, Shanghai, China) following the manufacturer's instructions. Tumor sections were incubated with primary antibodies (anti-CD31, 1:200, AF6191, Affinity, anti-CD34, 1:200, AF5149, Affinity, anti-IL-17A, 1:200, DF6127, Affinity, anti-VEGFA, 1:200, AF5131, Affinity) overnight at 4°C, followed by incubation with biotinylated secondary antibodies. Before microscopic analysis, streptavidin-biotin-peroxidase complex was added, and sections were incubated with 3,3'-diaminobenzidine (Maishin Bio, Fuzhou, China) at room temperature for 2 hours. Additionally, images were quantified using ImageJ software (National Institutes of Health, Bethesda, MD, USA). For microvascular density (MVD) quantification, CD31- and CD34-positive microvessels were counted in representative high-power fields from each tumor section. MVD was calculated as the number of positively stained microvessels per field or per analyzed area using ImageJ. The same thresholding and quantification criteria were applied across all groups.

Immunofluorescence

MDSC cells were stained using immunofluorescence staining methods. Following deparaffinization and hydration, antigen retrieval was performed using 10 mM Citrate Buffer (pH 6.0). Sections were then incubated with 5% bovine serum albumin at room temperature for 45 minutes. ITGAM antibody (1:200, DF2911, Proteintech, Affinity Biosciences) and Gr-1 antibody (1:100, #68590, CST) were incubated overnight. After washing, sections were incubated with corresponding fluorescently-labeled secondary antibodies (1:200, S0011, Affinity) for 60 minutes, followed by DAPI staining (D9542, Sigma-Aldrich, Merck KGaA, Darmstadt, Germany) for 10 minutes, and then washed with PBS and dried. Images were captured using a fluorescence microscope (Olympus, Tokyo, Japan) and analyzed with Image J software (National Institutes of Health).

Enzyme-Linked Immunosorbent Assay (ELISA)

Cytokine levels were measured using ELISA kits (IFN-γ, EK280HS-96, IL-10, EK310HS, iNOS, TNF-α, EK382HS, IL-17A, EK217, Arg-1, VEGFA, EK283) according to the manufacturer's guidelines. For serum samples, blood was collected from mice and centrifuged at 3000 rpm for 10 minutes at 4 °C to separate the serum, which was aliquoted and stored at −80 °C until analysis. Briefly, 100 μL of diluted antibody was added to each well of the ELISA plate and incubated at 37 °C for 1 hour. Then, 100 μL of biotinylated antibody was added and incubated in a 5% CO_2 incubator at 37 °C for another hour. The enzyme conjugate (100 μL) and substrate (100 μL) were mixed and incubated together in the incubator with 5% CO_2 at 37 °C for 30 minutes and 15 minutes, respectively. The reaction was terminated with 100 μL of stop solution, and the OD_{450} value was measured using an ELISA reader (model 680, Bio-Rad, Hercules, CA, USA).

In addition, frozen tumor tissues stored at –80 °C were homogenized in cold PBS containing protease inhibitors, followed by centrifugation at 12,000 × g for 15 minutes at 4 °C to collect supernatants. Cytokine concentrations (IFN-γ, TNF-α, IL-10, Arg-1, iNOS, IL-17A, VEGF) were determined using the same ELISA kits as above, according to the manufacturer's instructions. Total protein concentrations were measured using the BCA assay, and cytokine levels were normalized to protein content (pg/mg protein).

Statistical Analysis

Data were presented as mean ± standard deviation (SD) and analyzed using SPSS 20.0 (IBM Corp, Armonk, NY, USA) and GraphPad Prism 9.0 (GraphPad Software, Inc., San Diego, CA, USA). For comparisons among four groups, one-way analysis of variance (ANOVA) followed by Tukey's post hoc test was used. Tumor growth curves were analyzed using two-way repeated-measures ANOVA. The Kaplan-Meier method was used to estimate survival curves, and the Log rank test was applied to compare differences between groups. A P-value < 0.05 was considered statistically significant.

Results

Anlotinib Combined with PD-1/PD-L1-IN-9 Hydrochloride Suppresses Tumor Growth

To investigate the effects of anlotinib combined with a PD-1/PD-L1-IN-9 hydrochloride, we first assessed tumor growth and progression in CT26 tumor-bearing mice. The specific administration schemes for anlotinib and PD-1/PD-L1-IN -9 hydrochloride injections are shown in Figure 1A. We compared four groups: vehicle control, anlotinib monotherapy, PD-1/PD-L1-IN-9 hydrochloride monotherapy, and combination therapy. Initially, by measuring the terminal body weight of mice, we found that there were no significant changes in the terminal body weight of mice under different treatments (Figure 1B). Subsequently, by statistically analyzing the tumor weight and volume at the endpoint, we found that the combined treatment significantly reduced the tumor size and volume compared to the NC group and the individual treatment groups (Figures 1C–1E). At the same time, we measured and recorded tumor volume changes every 3 days during the treatment period (from day 1 to day 10). The statistics showed that the combined treatment group significantly inhibited tumor growth (Figure 1F). In addition, we monitored the survival of tumor-bearing mice receiving different treatments from day 0 to day 100. The treatment period lasted from day 1 to day 10, and after treatment, the survival cohort was followed until mice reached the end of observation, and euthanasia/death time and endpoint are listed in Supplementary Table S2. The statistics showed that the survival time of mice in the combined treatment group was significantly prolonged (Figure 1G). Additionally, we examined apoptosis in mouse tumor tissues. Western Blot results suggested that the combined treatment group had downregulated expression of Bcl-2 and increased expression of cleaved caspase-3 and Bax (Figure 1H), and the rate of TUNEL-positive staining increased in the combined treatment group (Figure 1I). These results indicate that anlotinib can enhance the antitumor effect of PD-1 inhibitors in CT26 tumor-bearing mice.

PD-1/PD-L1-IN-9 Hydrochloride Combined with Anlotinib Induces Neovascularization and Alleviates Hypoxia

Substantial evidence indicates that anti-angiogenic drugs can normalize the tumor vasculature system, alleviate tissue hypoxia, and thus improve the tumor immune microenvironment.[18] Given that anlotinib has previously been proven to exert strong anti-angiogenic effects in various tumor models,[19,20] we investigated the impact of anlotinib in both monotherapy and combined with PD-1/PD-L1-IN-9 hydrochloride on the progression of colorectal tumors. Studies have shown that IL-17A can promote neovascularization by activating the NF-κB signaling pathway, inducing the expression of vascular endothelial growth factor (VEGF) and matrix metalloproteinases (MMPs), as well as modulating the activity of endothelial and stromal cells.[21] We conducted immunohistochemical analysis to measure and quantify the levels of IL-17A and VEGF, finding that their expression levels significantly decreased after combined treatment (Figures 2A–2E). CD31 and CD34 are two common cell surface markers that play important roles in vasculogenesis, and the detection of CD31 and CD34 expression can assess the extent and activity of angiogenesis. Therefore, we

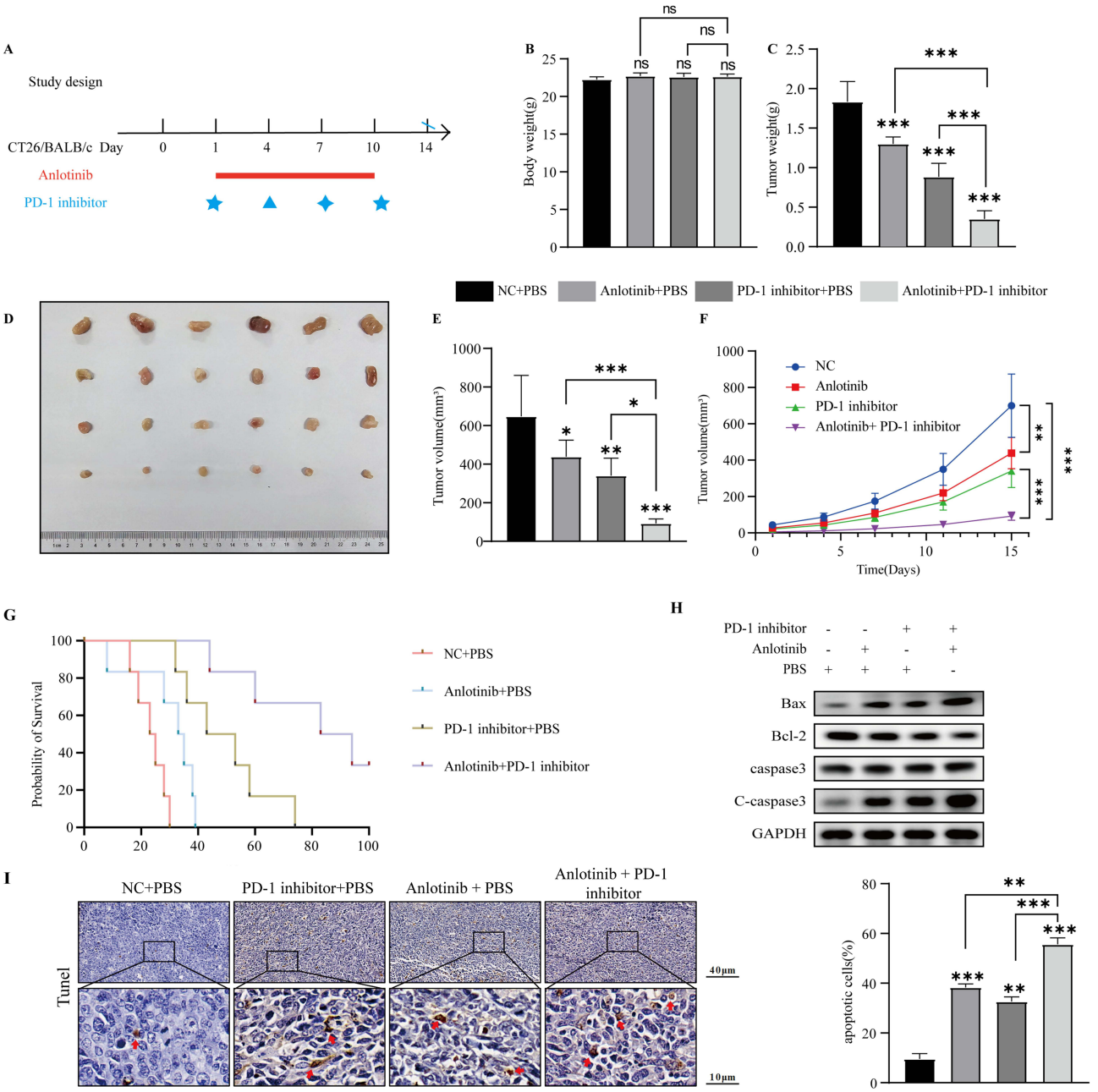

Figure 1 Anlotinib Combined with PD-1/PD-L1-IN-9 hydrochloride Significantly Suppresses Tumor Growth. (A) Schematic of the study design. The red bar indicates the duration of Anlotinib treatment (Days 1–10). Blue symbols indicate PD-1/PD-L1-IN-9 hydrochloride injection time points (Days 1, 4, 7, and 10), different shapes (star, triangle, diamond) are used only for visual distinction of injection days. (**B**). Changes in mouse body weight following different treatments (n=6). (**C**). Tumor weights in mice following different treatments (n=6). (**D**). Gross images of mouse tumors following different treatments. (**E**). Statistical chart of tumor volumes shown in panel D (n=6). (**F**). Growth curve of tumor volume, measured every 3 days (n=6). (**G**). Kaplan–Meier survival analysis of mice following different treatments (n=6). Survival was analyzed using the Kaplan–Meier method and compared with the Log rank test ($P < 0.001$ for combination vs control). (**H**). Western Blot analysis of apoptotic protein expression in tumor tissues under different treatments (n=3). (**I**). TUNEL staining results and statistical chart of tumor tissues from different treatment groups (scale = 40 μm), The areas indicated by the red arrows represent TUNEL-positive staining.

Notes: Data are presented as mean ± SD. Two-group comparisons were performed with Student's *t*-test. Multi-group comparisons were analyzed by one-way ANOVA followed by Tukey's post hoc test. Tumor growth curves were analyzed by two-way ANOVA. Survival curves were analyzed by the Kaplan–Meier method with Log rank test. (ns: not significant, *$P < 0.05$, **$P < 0.01$, ***$P < 0.001$ vs control unless otherwise indicated).

dynamically analyzed the expression of CD31 and CD34 through immunohistochemistry and calculated the ratio of microvessel density (MVD) to the area of the image using ImageJ software (Figures 2C–2F). Additionally, given the chronic hypoxia condition in the TME and literature indicating that HIF1-α promotes the formation of new blood vessels by upregulating the expression of various angiogenesis-related genes such as VEGF, thereby promoting endothelial cell

https://doi.org/10.2147/ITT.S597338

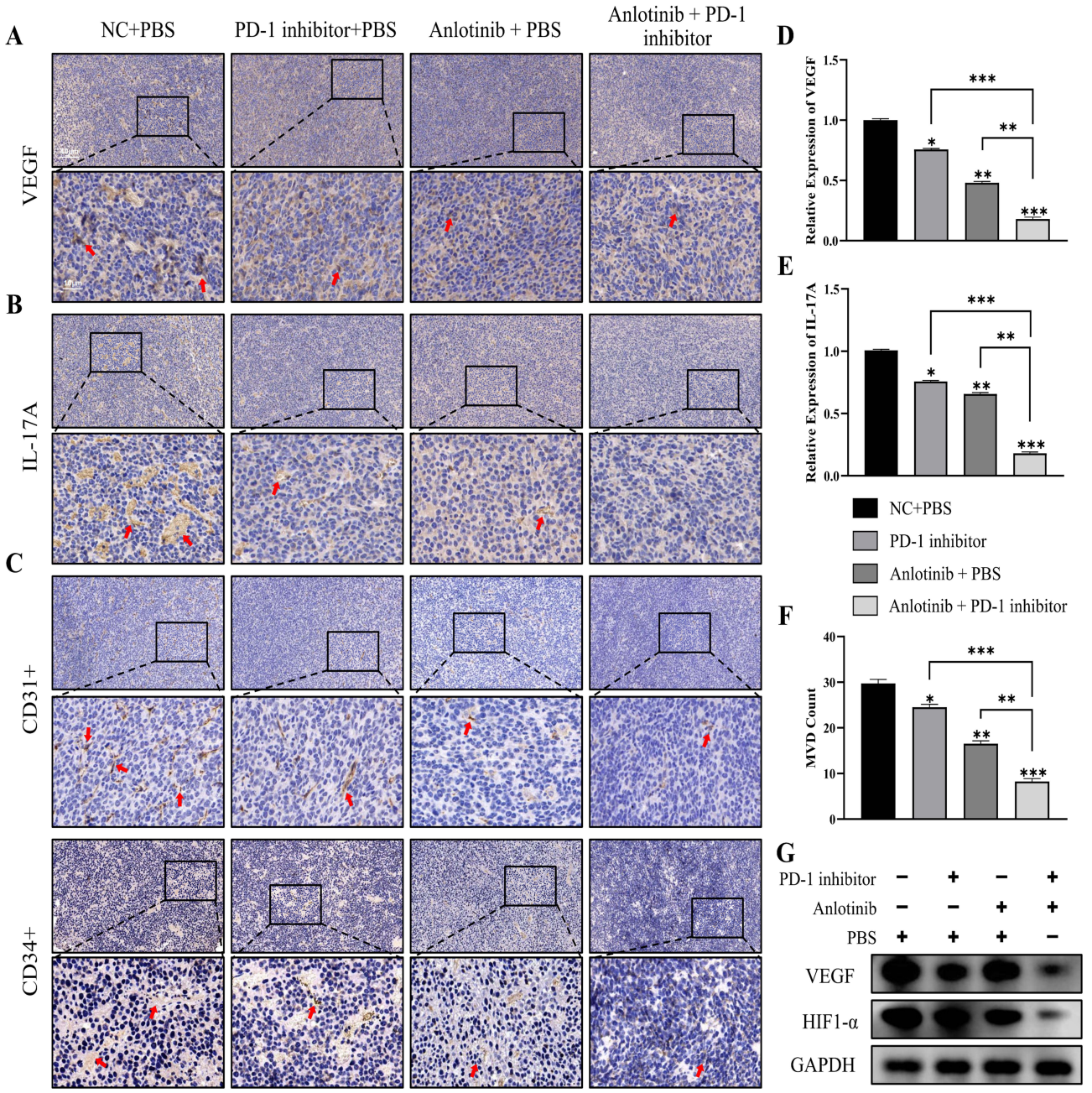

Figure 2 PD-1/PD-L1-IN-9 hydrochloride combined with anlotinib induces neovascularization and alleviates hypoxia (scale = 40 μm).(**A**). Immunohistochemical analysis of VEGF expression under different treatments. (**B**). Immunohistochemical detection of IL-17A expression. (**C**). Immunohistochemical analysis of the expression levels of vascular markers CD31 and CD34. The areas indicated by the red arrows represent TUNEL-positive staining. (**D** and **E**). Quantitative analysis of the expression levels of VEGF and IL-17A. F. Assessment of CD31+ and CD34+ numbers using ImageJ software to calculate MVD (*P < 0.05, **P < 0.01, ***P < 0.001 vs control unless otherwise indicated, n=3). (**G**). Western Blot analysis of VEGF and HIF1-α protein expression in tumor tissues under different treatments (n=3). Statistical analysis was performed using one-way ANOVA followed by Tukey's post hoc test.

proliferation and migration,[22,23] we examined the levels of HIF-α and VEGF in tumor tissues through Western Blot. We found that combined treatment significantly alleviated tissue hypoxia and suppressed the expression of VEGF (Figures 2G). Based on these results, it can be concluded that the combined treatment of anlotinib with a PD-1/PD-L1-IN-9 hydrochloride significantly alleviates tissue hypoxia, inhibits tumor angiogenesis, and induces the normalization of the remaining vessels.

https://doi.org/10.2147/ITT.S597338

PD-1/PD-L1-IN-9 Hydrochloride Combined with Anlotinib Reduces the Proportion of Immunosuppressive Cells

To explore the specific mechanisms through which the combined treatment suppresses tumor progression, we analyzed changes in immune cells within the tumor tissue. Initially, we examined the expression of MDSCs (Myeloid-Derived Suppressor Cells) through immunofluorescence. The results indicated that compared to monotherapy groups, the combined treatment group showed significantly reduced fluorescence intensity of MDSCs (Figures 3A–3E). Moreover, increasing evidence suggests that myeloid cells, namely Tumor-Associated Macrophages (TAMs), and lymphoid cells, such as FoxP3^{+} Regulatory T cells (Tregs), are major sources of immunosuppression within the Tumor Microenvironment(TME).[24,25] To further explore the impact of combined treatment on the tumor's immunosuppressive microenvironment, we assessed the levels of MDSCs, M2-type macrophages, and Tregs in the TME using flow cytometry. The results showed that the proportions of MDSCs, M2-type macrophages, and Tregs were significantly reduced in tumors treated with the combined therapy (Figures 3B–3F). These findings suggest that anlotinib may enhance the response to PD-1/PD-L1-IN-9 hydrochloride treatment by reducing the proportion of immunosuppressive cells within the TME, thereby inhibiting the progression of colorectal cancer.

PD-1/PD-L1-IN-9 Hydrochloride Combined with Anlotinib Increases Immune Lymphocyte Infiltration in Tumors

A recent study demonstrates that Anlotinib partially facilitates tumor neovascularization by upregulating CD4+ T cells, thereby reprogramming the immunosuppressive tumor microenvironment into an immunostimulatory one and significantly inhibiting tumor growth [18]. Additionally, the infiltration of CD8+ T lymphocytes within tumors serves as a prognostic factor for the efficacy of immunotherapy. To assess the changes in CD4+ and CD8+ T cells within tumor tissues following various treatments, we prepared single-cell suspensions of the tumors and analyzed them using flow cytometry. The results revealed that, compared to monotherapy, the combination therapy enhanced the infiltration of CD8+ T cells at the tumor site and improved the tumor microenvironment. Compared with the control group, the percentage of CD4+ T cells in the combination group was significantly increased; however, when compared with the PD-1/PD-L1-IN-9 hydrochloride monotherapy group, it was significantly decreased. Notably, no obvious synergistic effect was observed in the combination group (Figure 4A–4E). Moreover, we examined the expression of PD-1 on the surface of CD4+ and CD8+ T cells. The findings showed that, relative to the control group, combination therapy significantly reduced PD-1 expression on both CD4+ and CD8+ T cells (Figure 4C–4E). These findings suggest that anlotinib may enhance the efficacy of PD-1/PD-L1-IN-9 hydrochloride treatment by upregulating the proportion of immune effector cells in the TME.

PD-1/PD-L1-IN-9 Hydrochloride Combined with Anlotinib Jointly Improves the Immune Microenvironment

Cytokines play a crucial role in the crosstalk between immune cells and tumor cells.[26] To determine the activity and function of immune cells, we first evaluated the levels of immune stimulatory factors (IFN-γ, TNF-α) and immune suppressive factors (IL-17, IL-10, ARG1, VEGF, and iNOS) in the peripheral blood through ELISA (Figure 5A and 5B). The results showed that in the combination treatment group, IL-10, ARG1, IL-17, VEGF, and iNOS were downregulated, whereas IFN-γ and TNF-α were upregulated. To further validate whether these systemic changes reflect the local tumor microenvironment, we additionally measured cytokine levels in tumor tissue homogenates by ELISA. Consistently, IFN-γ and TNF-α were elevated, while IL-10, ARG1, IL-17, VEGF, and iNOS were reduced in tumor tissues of the combination group, confirming that anlotinib plus PD-1/PD-L1-IN-9 hydrochloride remodels both systemic and intratumoral immune profiles. Together, these findings suggest that the combination therapy improves the immune microenvironment at multiple levels, thereby enhancing the efficacy of PD-1 blockade.

Discussion

Given the established fact that immune evasion promotes tumor progression, active immunotherapy has emerged as the third major pillar alongside chemotherapy and targeted therapy. Cancer immunotherapy aims to activate the host immune system to selectively eliminate malignant cells without harming normal body tissues. However, most immunotherapies have not achieved their expected antitumor effects clinically, with relatively low benefit rates.[27] Previous data have shown that anti-angiogenic therapy targets the tumor vascular system to inhibit tumor growth and alleviate tumor burden.[28] Despite certain clinical effects of anti-angiogenic targeted drugs and immunotherapy in tumor treatment, neither has shown a strong and durable clinical response when used as a single agent for colorectal cancer. Moreover, an increasing number of studies have indicated that anti-angiogenic targeted drugs can induce tumor neovascularization, reduce vascular density to alleviate tumor burden, and increase the infiltration of immune effector cells to transform the immunosuppressive TME, thereby enhancing the efficacy of cancer immunotherapy.[29]

In this study, we demonstrated the effects of combined administration of anlotinib and PD-1 inhibitors on vascular structure and function, antitumor immunity, tumor growth, and survival rates in a subcutaneous tumor model in BALB/c

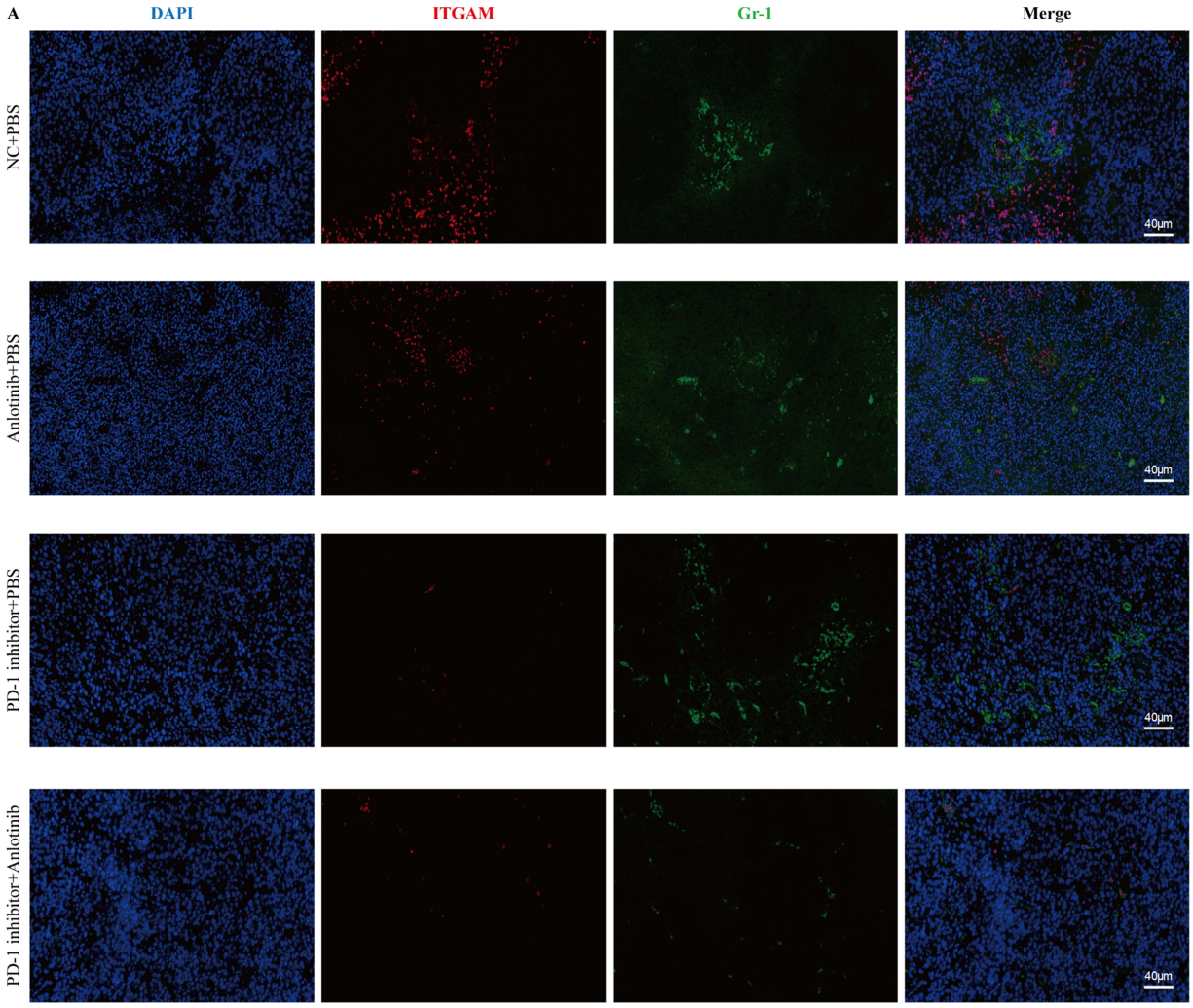

Figure 3 PD-1/PD-L1-IN-9 hydrochloride Combined with Anlotinib Reduces the Proportion of Immunosuppressive Cells. (**A**). Expression differences of MDSCs under different treatments detected using immunofluorescence technology and labeled with ITGAM and Gr-1. DAPI (blue), ITGAM (red), Gr-1 (green). (scale = 40 μm). (**B**). The percentage of MDSCs within the tumor using flow cytometry. (**C**). The percentage of M2-type macrophages within the tumor using flow cytometry. (**D**). The percentage of Tregs within the tumor using flow cytometry. (**E**). Quantitative analysis of the immunofluorescence images from (**A**). (**F**). Quantitative analysis of the flow cytometry results from (**B**–**D**). (*P < 0.05, **P < 0.01, ***P < 0.001 vs control unless otherwise indicated, n=3). Statistical analysis was performed using one-way ANOVA followed by Tukey's post hoc test.

https://doi.org/10.2147/ITT.S597338

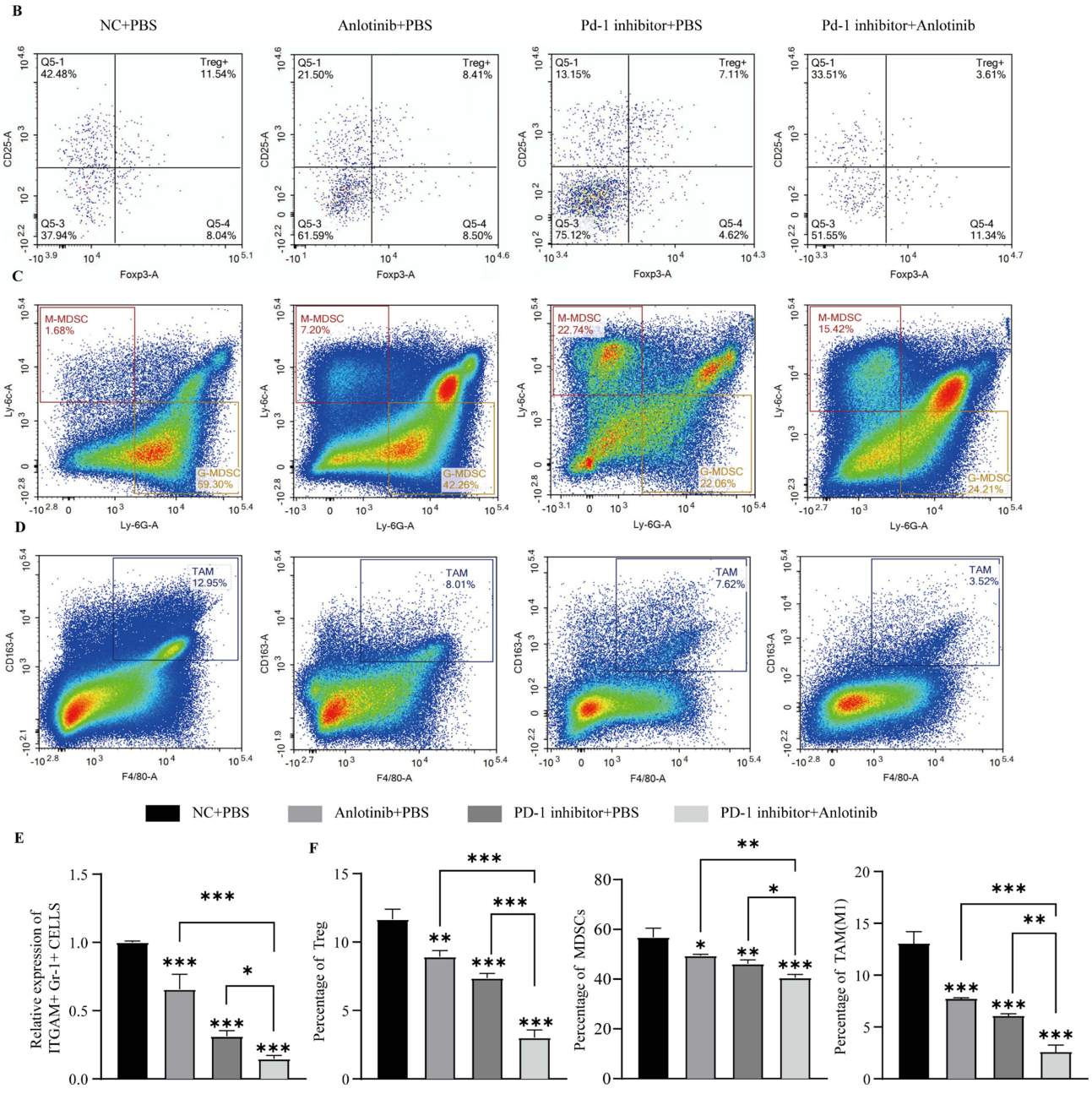

Figure 3 Continued.

mice. PD-1 inhibitors was a small-molecule inhibitor that selectively blocks the PD-1/PD-L1 interaction, thereby preventing inhibitory signaling and restoring effector T-cell function. This compound has been reported in preclinical studies to effectively disrupt PD-1/PD-L1 binding and enhance antitumor immune responses.[30] Several basic studies have found that after effectively inhibiting the classical VEGFA pathway, tumor cells often activate a variety of compensatory "bypass activation" pathways, such as VEGFC, TGF, and FGF pathways, worsening the biological behavior of tumor cells and leading to rapid "rebound" of tumors and even increased invasiveness and metastatic potential post-treatment.[31–34] Therefore, the activation of bypass pathways in tumor vascular endothelial cells (ECs) after inhibiting the main angiogenesis signaling pathways has become an important cause of resistance. The new generation of anti-angiogenic drug anlotinib targets angiogenesis pathways including VEGFR, FGFR, and PDGFR, as well as the stem

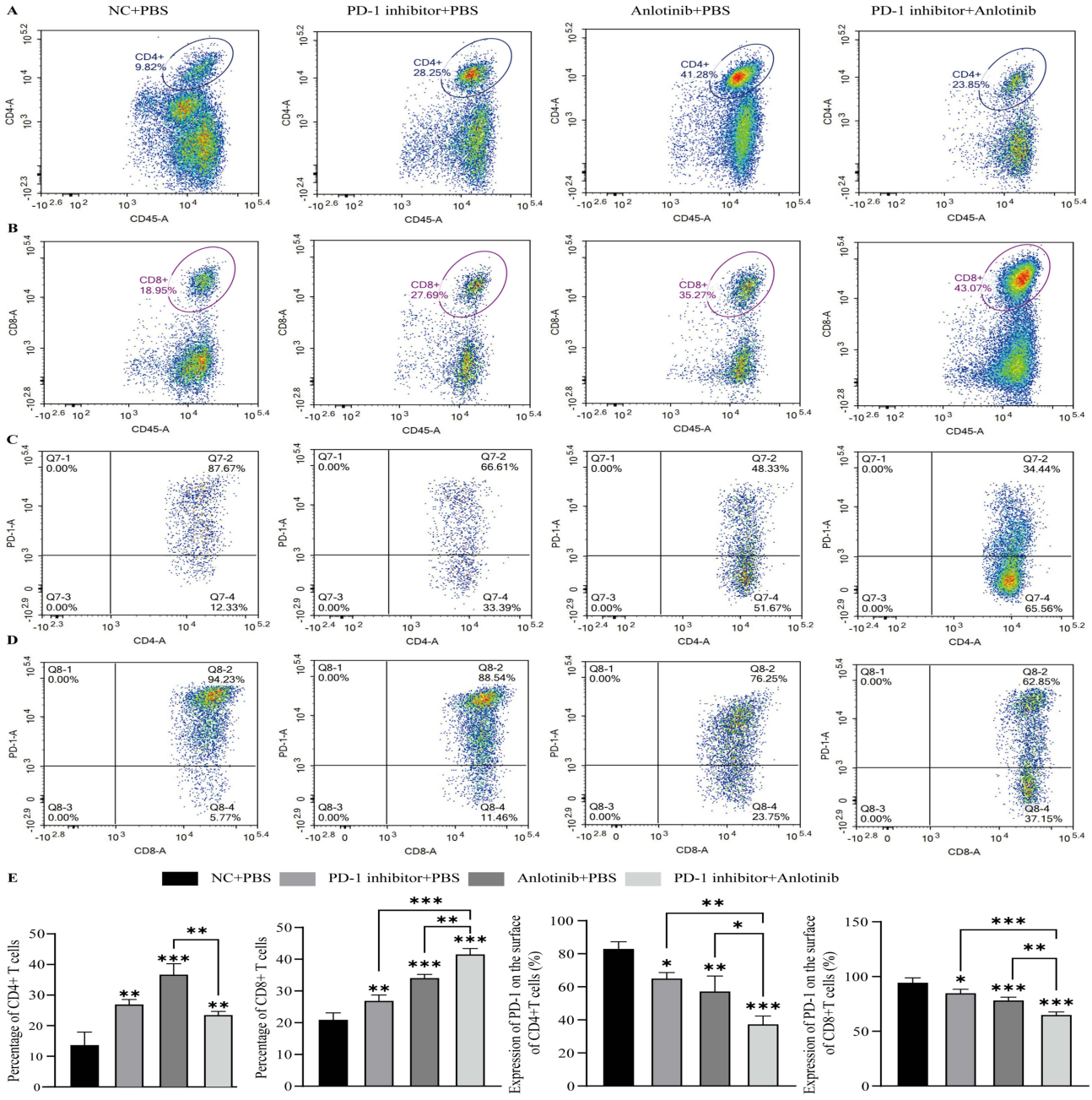

Figure 4 PD-1/PD-L1-IN-9 hydrochloride Combined with Anlotinib Increases Immune Lymphocyte Infiltration in Tumors.(**A** and **B**). Detection of CD4+ T and CD8+ T cells in tumors under different treatments using flow cytometry. (**C** and **D**). Expression of PD-1 on the surface of CD4+ T cells and CD8+ T cells under different treatments. (**E**). Statistical analysis of the above results (*P < 0.05, **P < 0.01, ***P < 0.001 vs control unless otherwise indicated, n=6). All flow cytometry percentages are shown relative to $CD45^+$ leukocytes. Statistical analysis was performed using one-way ANOVA followed by Tukey's post hoc test.

cell factor receptor c-KIT.[12] Its multi-target mechanism significantly improves clinical treatment effects, prolonging PFS and OS in patients with advanced NSCLC, and ending the history of drug-resistant lung cancer patients.[13] A study showed that patients with advanced LUAD carrying KRAS mutations, after progressing through multiple lines of chemotherapy and radiotherapy, received anlotinib treatment, ultimately achieving a PFS of 21 months and an OS of 5.5 years.[35]

In our study, anlotinib combined with PD-1/PD-L1-IN-9 hydrochloride treatment significantly inhibited colorectal cancer growth, extended the survival period of BALB/c subcutaneous tumor-bearing mice, and improved the tumor immune suppressive microenvironment, promoting its response to immunotherapy. Furthermore, studies have shown that

https://doi.org/10.2147/ITT.S597338

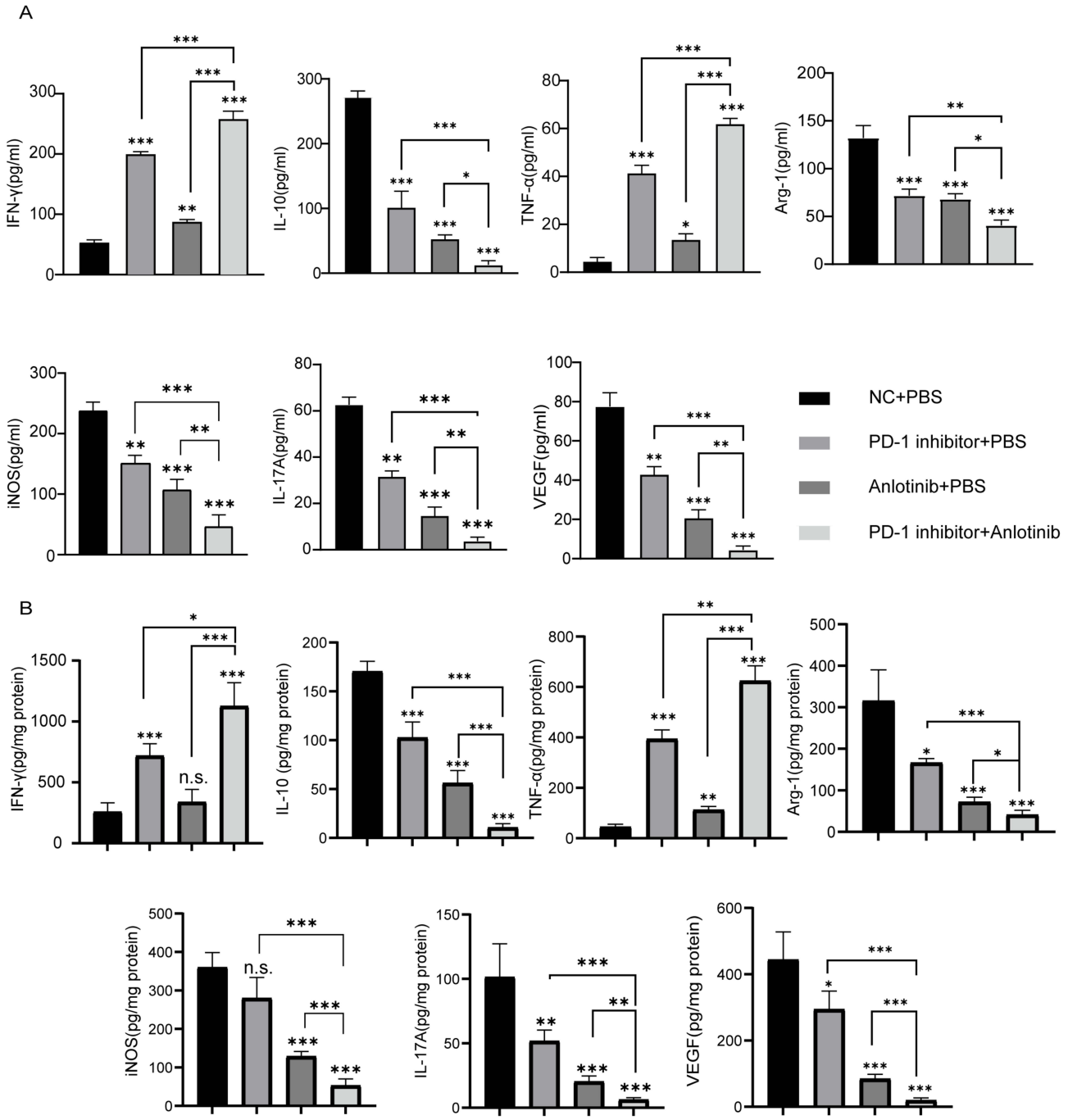

Figure 5 PD-1/PD-L1-IN-9 hydrochloride Combined with Anlotinib Jointly Improves the Immune Microenvironment.(**A**) ELISA analysis of cytokine expression (IFN-γ, IL-10, TNF-α, Arg-1, iNOS, IL-17A, VEGF) in mouse serum.(**B**). ELISA analysis of cytokine expression (IFN-γ, IL-10, TNF-α, Arg-1, iNOS, IL-17A, VEGF) in tumor tissue homogenates.

Notes: (*P < 0.05, **P < 0.01, ***P < 0.001 vs control unless otherwise indicated; n = 6). Statistical analysis was performed using one-way ANOVA followed by Tukey's post hoc test.

VEGF can promote local and systemic immune suppression by targeting angiogenesis to cause hypoxia and low pH values in the TME.[36] Moreover, an increasing number of preclinical studies have shown that when combined with immunotherapy, anti-angiogenic drugs can enhance antitumor efficacy by changing the infiltration of lymphocytes or macrophages in a series of tumor immune microenvironments.[37,38] The experimental data indicate that the combination of anlotinib and PD-1 inhibitors effectively reduces the expression of VEGFA, greatly alleviates tissue hypoxia, and increases the percentage of CD8+ T cells within the tumor to improve the immunosuppressive microenvironment.

Evidence suggests that activated CD8+ T cells may also promote tumor neovascularization.[39] Therefore, anlotinib and activated CD8+ T cells are likely to work synergistically to induce tumor neovascularization. More importantly, compared to monotherapy, combination therapy significantly reduced the proportion of immunosuppressive cells such as MDSCs, M2-type macrophages, and Tregs, indicating its potential to re-activate the immune system and suppress the formation of an immunosuppressive microenvironment. Mechanistically, our findings suggest that neovascularization and immune remodeling may interact to create a positive feedback loop. By transiently normalizing abnormal tumor vasculature, anlotinib alleviates hypoxia and improves perfusion, which facilitates the infiltration and function of effector $CD8^+$ T cells. In turn, the increased presence of activated $CD8^+$ T cells, together with the reduction of immunosuppressive cells (MDSCs, Tregs, M2 macrophages), may contribute to sustaining neovascularization through cytokine regulation. This reciprocal interaction provides a plausible explanation for the synergistic effect observed in our study and highlights the therapeutic rationale of combining anti-angiogenic therapy with PD-1 blockade in MSS colorectal cancer.[14,40]

Next, we determined the levels of cytokines related to the activity and function of immune cells. The combined treatment group showed the highest IFN-γ levels. It has been reported that IFN-γ is mainly secreted by activated lymphocytes such as $CD4^+$ and $CD8^+$ T cells, γδ-T cells, and NK and NKT cells.[41,42] Previous studies have also described various antitumor effects of IFN-γ, including regulating antigen presentation, promoting inflammatory and chemotactic signals, activating and polarizing responsive leukocytes, recruiting effector leukocytes, as well as direct antiproliferative and anti-angiogenic effects.[43] Our data demonstrate elevated IFN-γ levels following combination therapy, consistent with these known immune-activating functions. In the immune response, especially in cell-mediated immunity, activated T cells release TNF-α to regulate and enhance immune responses.[44] Furthermore, inducible nitric oxide synthase (iNOS) suppresses the function of immune cells by producing nitric oxide (NO), thereby aiding tumors in evading immune surveillance.[45] We also measured the levels of Arg-1 and IL-10 in mouse tumor tissues, finding that Arg-1 was significantly reduced in the combined therapy. IL-10 can inhibit the activity of immune cells, such as inhibiting the antigen presentation and pro-inflammatory effects of macrophages and dendritic cells, as well as inhibiting the activity of CD4+ and CD8+ T cells, reducing the T cells' attack on tumors.[46] It has been reported that increased levels of Arg-1 expressed by MDSCs mediate the depletion of L-arginine in the TME, leading to T cell cycle arrest and loss of T cell efficacy, due to the downregulation of TCR zeta chain expression.[47] Interestingly, besides its immunosuppressive function, IL-17A, like VEGF, also promotes neovascularization.[48] In our study, both serum and tumor tissue analyses consistently showed increased IFN-γ and TNF-α and decreased IL-10, ARG1, IL-17, VEGF, and iNOS in the combination group, indicating that the systemic and local immune environments were improved in parallel. In summary, combined therapy mediates the crosstalk between tumor cells and immune cells by affecting different cytokine levels, improving the tumor suppressive microenvironment.

In interpreting our flow cytometry data, it is important to note that PD-1 expression on $CD8^+$ T cells can reflect distinct biological states. While PD-1 may indicate activation during early priming, sustained high expression within the tumor microenvironment is widely associated with T-cell exhaustion, characterized by impaired proliferation and reduced cytokine production.[49–51] Consistent with this concept, blockade of PD-1 has been shown to reinvigorate exhausted $CD8^+$ T cells and restore effector functions.[52,53] In our study, the observed decline in $PD\text{-}1^+CD4^+$ and $PD\text{-}1^+CD8^+$ subsets following combination treatment likely reflects partial reversal of exhaustion rather than a loss of activation. Although tumor antigen specificity was not directly tested, the analysis was performed on $CD45^+$ tumor-infiltrating lymphocytes, which predominantly represent tumor-reactive T cells. Moreover, the neovascularization induced by anlotinib may facilitate the recruitment of peripheral effector T cells into the tumor, potentially in parallel with local clonal expansion. These findings together suggest that the combination strategy not only increases effector T-cell abundance but also improves their functional quality within the tumor microenvironment.

However, our study has some limitations. First, the relatively small sample size may limit the statistical robustness of our findings; this number was chosen based on ethical considerations to minimize animal use and is consistent with many previous preclinical studies. Second, we employed a subcutaneous rather than an orthotopic colorectal cancer model, which may not fully recapitulate the native tumor microenvironment, particularly with respect to angiogenesis and immune cell infiltration[54] We acknowledge that the lack of an orthotopic model represents a limitation, and future studies

will validate our findings in orthotopically implanted tumors to strengthen their translational relevance. Third, only selected immune cell subsets ($CD4^+$, $CD8^+$ T cells, Tregs, MDSCs, and M2 TAMs) were analyzed, whereas other relevant populations such as NK cells and dendritic cells were not assessed. Furthermore, the lack of longitudinal body weight monitoring represents another limitation; while animals were assessed daily based on humane endpoints, the absence of continuous weight data limits the comprehensive evaluation of treatment-related toxicity and distress. Finally, we did not evaluate the impact on tumor recurrence, and the precise molecular pathways underlying the observed changes in the tumor immune microenvironment remain to be elucidated. Despite these limitations, our data suggest that anlotinib combined with PD-1/PD-L1-IN-9 hydrochloride immunotherapy may represent a promising synergistic treatment for CRC patients. While our research holds significant clinical relevance, the combination of anti-angiogenic therapy with PD-1 inhibition warrants further evaluation in clinical trials.

Conclusion

This study investigated the synergistic antitumor effects of anlotinib in combination with a PD-1 inhibitor using a murine subcutaneous tumor model, and the results demonstrated significant suppression of colorectal cancer growth along with remarkable improvement of the tumor immune microenvironment. Specifically, the combination therapy notably reduced the proportion of key immunosuppressive cell populations, including myeloid-derived suppressor cells (MDSCs), M2-type macrophages, and regulatory T cells (Tregs). Moreover, it modulated cytokine levels to mediate the crosstalk between tumor cells and immune cells, thereby reshaping the immunosuppressive tumor microenvironment into a more immunopermissive state. Collectively, this study provides robust preclinical evidence that the combination of anlotinib and PD-1/PD-L1-IN-9 hydrochloride enhances antitumor activity through multiple complementary mechanisms—specifically by regulating angiogenesis, alleviating tumor hypoxia, and remodeling the tumor immune microenvironment. Nevertheless, further clinical validation is required to confirm these preclinical findings and translate them into potential therapeutic strategies for colorectal cancer.

Data Sharing Statement

All data generated or analyzed during this study are included in this published article.

Ethics Approval and Consent to Participate

All procedures involving animal care and use were approved by the Experimental Animal Ethics Committee of the Zhongyan Zichuang (Beijing) Biotechnology Co., Ltd and followed the National Policy on the Use of Laboratory Animals (Ethics number ZYZC202402011S).

Consent for Publication

All authors agreed to this publication.

Acknowledgments

We would like to thank all laboratory members for their discussion of this manuscript.

Author Contributions

All authors made a significant contribution to the work reported, whether that is in the conception, study design, execution, acquisition of data, analysis and interpretation, or in all these areas; took part in drafting, revising or critically reviewing the article; gave final approval of the version to be published; have agreed on the journal to which the article has been submitted; and agree to be accountable for all aspects of the work.

Funding

This project was financially supported by the Key Construction Program of the National "135" Project (2017YFC0112102, 2017YFC0112104).

Disclosure

The authors declare that they have no competing interests in this work.

References

1. Sung H, Ferlay J, Siegel RL, et al. Global Cancer Statistics 2020: GLOBOCAN estimates of incidence and mortality worldwide for 36 cancers in 185 countries. *Ca a Cancer J Clinicians*. 2021;71(3):209–249. doi:10.3322/caac.21660
2. Kuipers EJ, Grady WM, Lieberman D, et al. Colorectal cancer. *Nat Rev Dis Primers*. 2015;1:15065. doi:10.1038/nrdp.2015.65
3. Yoshino T, Arnold D, Taniguchi H, et al. Pan-Asian adapted ESMO consensus guidelines for the management of patients with metastatic colorectal cancer: a JSMO-ESMO initiative endorsed by CSCO, KACO, MOS, SSO and TOS. *Ann Oncol*. 2018;29:44–70. doi:10.1093/annonc/mdx738
4. Pardoll DM. The blockade of immune checkpoints in cancer immunotherapy. *Nat Rev Cancer*. 2012;12:252–264. doi:10.1038/nrc3239
5. Ciardiello D, Vitiello PP, Cardone C, et al. Immunotherapy of colorectal cancer: challenges for therapeutic efficacy. *Cancer Treat Rev*. 2019;76:22–32. doi:10.1016/j.ctrv.2019.04.003
6. Hermel DJ, Sigal D. The emerging role of checkpoint inhibition in microsatellite stable colorectal cancer. *J Pers Med*. 2019;9:5. doi:10.3390/jpm9010005
7. Jain RK. Antiangiogenesis strategies revisited: from starving tumors to alleviating hypoxia. *Cancer Cell*. 2014. 26;605–622. doi:10.1016/j.ccell.2014.10.006
8. Jain RK. Normalizing tumor microenvironment to treat cancer: bench to bedside to biomarkers. *J Clin Oncol*. 2013;31:2205–2218. doi:10.1200/JCO.2012.46.3653
9. Georganaki M, van Hooren L, Dimberg A. Vascular targeting to increase the efficiency of immune checkpoint blockade in cancer. *Front Immunol*. 2018;9:3081. doi:10.3389/fimmu.2018.03081
10. Shrimali RK, Yu Z, Theoret MR, Chinnasamy D, Restifo NP, Rosenberg SA. Antiangiogenic agents can increase lymphocyte infiltration into tumor and enhance the effectiveness of adoptive immunotherapy of cancer. *Cancer Res*. 2010;70(15):6171–6180. doi:10.1158/0008-5472.CAN-10-0153
11. Fukumura D, Jain RK. Tumor microenvironment abnormalities: causes, consequences, and strategies to normalize. *J Cell Biochem*. 2007;101(4):937–949. doi:10.1002/jcb.21187
12. Shen G, Zheng F, Ren D, et al. Anlotinib: a novel multi-targeting tyrosine kinase inhibitor in clinical development. *J Hematol Oncol*. 2018;11(1):120. doi:10.1186/s13045-018-0664-7
13. Han B, Li K, Wang Q, et al. Effect of anlotinib as a third-line or further treatment on overall survival of patients with advanced non–small cell lung cancer. *JAMA Oncol*. 2018;4:1569. doi:10.1001/jamaoncol.2018.3039
14. Fan P, Qiang H, Liu Z, et al. Effective low-dose Anlotinib induces long-term tumor vascular normalization and improves anti-PD-1 therapy. *Front Immunol*. 2022;13:937924. doi:10.3389/fimmu.2022.937924
15. Yu L, Xu J, Qiao R, Han B, Zhong H, Zhong R. Efficacy and safety of anlotinib combined with PD-1/PD-L1 inhibitors as second-line and subsequent therapy in advanced small-cell lung cancer. *Cancer Med*. 2023;12:5372–5383. doi:10.1002/cam4.5360
16. Liu Q, Chen X, Qi M, et al. Combined cryoablation and PD-1 inhibitor synergistically enhance antitumor immune responses in Lewis lung adenocarcinoma mice via the PI3K/AKT/mTOR pathway. *Biochim Biophys Acta Mol Basis Dis*. 2024;1870:167262. doi:10.1016/j.bbadis.2024.167262
17. Neco P, Torrente AG, Mesirca P, et al. Paradoxical effect of increased diastolic ca^{2+} release and decreased sinoatrial node activity in a mouse model of catecholaminergic polymorphic ventricular tachycardia. *Circulation*. 2012;126:392–401. doi:10.1161/CIRCULATIONAHA.111.075382
18. Huang Y, Goel S, Duda DG, Fukumura D, Jain RK. Vascular Normalization as an Emerging Strategy to Enhance Cancer Immunotherapy. *Cancer Res*. 2013;73:2943–2948. doi:10.1158/0008-5472.CAN-12-4354
19. Yuan M, Zhai Y, Men Y, et al. Anlotinib enhances the antitumor activity of high-dose irradiation combined with anti-pd-l1 by potentiating the tumor immune microenvironment in murine lung cancer. *Oxid Med Cell Longev*. 2022;2022. 5479491. doi:10.1155/2022/5479491
20. Su Y, Luo B, Lu Y, et al. Anlotinib induces a t cell–inflamed tumor microenvironment by facilitating vessel normalization and enhances the efficacy of pd-1 checkpoint blockade in neuroblastoma. *Clin Cancer Res*. 2022;28:793–809. doi:10.1158/1078-0432.CCR-21-2241
21. Shibabaw T, Teferi B, Ayelign B. The role of Th-17 cells and IL-17 in the metastatic spread of breast cancer: as a means of prognosis and therapeutic target. *Front Immunol*. 2023;14:1094823. doi:10.3389/fimmu.2023.1094823
22. Huang Y, Wang X, Lin H. The hypoxic microenvironment: a driving force for heterotopic ossification progression. *Cell Commun Signal*. 2020;18:10–20. doi:10.1186/s12964-020-0509-1
23. Wei X, Chen Y, Jiang X, et al. Mechanisms of vasculogenic mimicry in hypoxic tumor microenvironments. *Mol Cancer*. 2021;20:7. doi:10.1186/s12943-020-01288-1
24. Hanahan D, Coussens LM. Accessories to the crime: functions of cells recruited to the tumor microenvironment. *Cancer Cell*. 2012;21:309–322. doi:10.1016/j.ccr.2012.02.022
25. Sica A, Bronte V. Altered macrophage differentiation and immune dysfunction in tumor development. *J Clin Invest*. 2007;117:1155–1166. doi:10.1172/JCI31422
26. Zhao S, Ren S, Jiang T, et al. Low-Dose Apatinib Optimizes Tumor Microenvironment and Potentiates Antitumor Effect of PD-1/PD-L1 Blockade in Lung Cancer. *Cancer Immunol Res*. 2019;7:630. doi:10.1158/2326-6066.CIR-17-0640
27. Quezada SA, Peggs KS, Simpson TR, Allison JP. Shifting the equilibrium in cancer immunoediting: from tumor tolerance to eradication. *Immunol Rev*. 2011;241:104–118. doi:10.1111/j.1600-065X.2011.01007.x
28. Goel S, Duda DG, Xu L, et al. Normalization of the vasculature for treatment of cancer and other diseases. *Physiol Rev*. 2011;91:1071–1121. doi:10.1152/physrev.00038.2010
29. Huang Y, Yuan J, Righi E, et al. Vascular normalizing doses of antiangiogenic treatment reprogram the immunosuppressive tumor microenvironment and enhance immunotherapy. *Proceedings of the National Academy of Sciences - PNAS* (2012) **109**: 17561–17566. doi:10.1073/pnas.1215397109.
30. Wang T, Cai S, Wang M, et al. Novel biphenyl pyridines as potent small-molecule inhibitors targeting the programmed cell death-1/programmed cell death-ligand 1 interaction. *J Med Chem*. 2021;64:7390–7403. doi:10.1021/acs.jmedchem.1c00010

31. Rahbari NN, Kedrin D, Incio J, et al. Anti-VEGF therapy induces ECM remodeling and mechanical barriers to therapy in colorectal cancer liver metastases. *Sci Transl Med*. 2016;8:135r–360r. doi:10.1126/scitranslmed.aaf5219
32. Michaelsen SR, Staberg M, Pedersen H, et al. VEGF-C sustains VEGFR2 activation under bevacizumab therapy and promotes glioblastoma maintenance. *Neuro-Oncology*. 2018;20:1462–1474. doi:10.1093/neuonc/noy103
33. Qian C, Pezzella F. Tumor vasculature: a sally port for inhibiting cancer cell spreading. *Cancer Commun*. 2018;38:52. doi:10.1186/s40880-018-0322-z
34. Vilà N, Coblentz J, Moreira-Neto C, Bravo-Filho V, Zoroquiain P, Burnier JMN. Pretreatment of RPE Cells with Lutein Can Mitigate Bevacizumab-Induced Increases in Angiogenin and bFGF. *Ophthalmic Res*. 2017;57:48–53. doi:10.1159/000449252
35. Su Y, Meng Z, Xu X, et al. A case report of advanced lung adenocarcinoma harboring kras mutation treated with anlotinib. *Zhongguo Fei Ai Za Zhi*. 2018;21:428–430. doi:10.3779/j.issn.1009-3419.2018.05.13
36. Fukumura D, Kloepper J, Amoozgar Z, Duda DG, Jain RK. Enhancing cancer immunotherapy using antiangiogenics: opportunities and challenges. *Nat Rev Clin Oncol*. 2018;15:325–340. doi:10.1038/nrclinonc.2018.29
37. Huang Y, Kim BYS, Chan CK, Hahn SM, Weissman IL, Jiang W. Improving immune–vascular crosstalk for cancer immunotherapy. *Nat Rev Immunol*. 2018;18:195–203. doi:10.1038/nri.2017.145
38. Allen E, Jabouille A, Rivera LB, et al. Combined antiangiogenic and anti-PD-L1 therapy stimulates tumor immunity through HEV formation. *Sci Transl Med*. 2017:9. doi:10.1126/scitranslmed.aak9679.
39. Zheng X, Fang Z, Liu X, et al. Increased vessel perfusion predicts the efficacy of immune checkpoint blockade. *J Clin Invest*. 2018;128:2104–2115. doi:10.1172/JCI96582
40. Lee WS, Yang H, Chon HJ, Kim C. Combination of anti-angiogenic therapy and immune checkpoint blockade normalizes vascular-immune crosstalk to potentiate cancer immunity. *Exp Mol Med*. 2020;52:1475–1485. doi:10.1038/s12276-020-00500-y
41. Matsushita H, Hosoi A, Ueha S, et al. Cytotoxic T lymphocytes block tumor growth both by lytic activity and IFNgamma-dependent cell-cycle arrest. *Cancer Immunol Res*. 2015;3:26–36. doi:10.1158/2326-6066.CIR-14-0098
42. Gao Y, Yang W, Pan M, et al. Gamma delta T cells provide an early source of interferon gamma in tumor immunity. *J Exp Med*. 2003;198:433–442. doi:10.1084/jem.20030584
43. Burke JD, Young HA. IFN-gamma: a cytokine at the right time, is in the right place. *Semin Immunol*. 2019;43:101280. doi:10.1016/j.smim.2019.05.002
44. Kasprzak A. The Role of Tumor Microenvironment Cells in Colorectal Cancer (CRC) Cachexia. *Int J Mol Sci*. 2021;22:1565. doi:10.3390/ijms22041565
45. Kashfi K, Kannikal J, Nath N. Macrophage reprogramming and cancer therapeutics: role of inos-derived NO. *Cells*. 2021;10:3194. doi:10.3390/cells10113194
46. Wu AA, Drake V, Huang H, Chiu S, Zheng L. Reprogramming the tumor microenvironment: tumor-induced immunosuppressive factors paralyze T cells. *Oncoimmunology*. 2015;4:e1016700. doi:10.1080/2162402X.2015.1016700
47. Weber R, Groth C, Lasser S, et al. IL-6 as a major regulator of MDSC activity and possible target for cancer immunotherapy. *Cell Immunol*. 2021;359:104254. doi:10.1016/j.cellimm.2020.104254
48. Chung AS, Wu X, Zhuang G, et al. An interleukin-17-mediated paracrine network promotes tumor resistance to anti-angiogenic therapy. *Nat Med*. 2013;19:1114–1123. doi:10.1038/nm.3291
49. Dolina JS, Van Braeckel-Budimir N, Thomas GD, Salek-Ardakani S. CD8(+) T Cell Exhaustion in Cancer. *Front Immunol*. 2021;12:715234. doi:10.3389/fimmu.2021.715234
50. Wu X, Zhang H, Xing Q, et al. PD-1(+) CD8(+) T cells are exhausted in tumours and functional in draining lymph nodes of colorectal cancer patients. *Br J Cancer*. 2014;111:1391–1399. doi:10.1038/bjc.2014.416
51. Ma J, Zheng B, Goswami S, et al. PD1(Hi) CD8(+) T cells correlate with exhausted signature and poor clinical outcome in hepatocellular carcinoma. *J Immunother Cancer*. 2019;7:331. doi:10.1186/s40425-019-0814-7
52. Lee J, Ahn E, Kissick HT, Ahmed R. Reinvigorating exhausted t cells by blockade of the pd-1 pathway. *For Immunopathol Dis Therap*. 2015;6:7–17. doi:10.1615/ForumImmunDisTher.2015014188
53. Ahn E, Araki K, Hashimoto M, et al. Role of PD-1 during effector CD8 T cell differentiation. *Proc Natl Acad Sci U S A*. 2018;115:4749–4754. doi:10.1073/pnas.1718217115
54. Gould SE, Junttila MR, de Sauvage FJ. Translational value of mouse models in oncology drug development. *Nat Med*. 2015;21:431–439. doi:10.1038/nm.3853

ImmunoTargets and Therapy

Dovepress
Taylor & Francis Group

Publish your work in this journal

ImmunoTargets and Therapy is an international, peer-reviewed open access journal focusing on the immunological basis of diseases, potential targets for immune based therapy and treatment protocols employed to improve patient management. Basic immunology and physiology of the immune system in health, and disease will be also covered. In addition, the journal will focus on the impact of management programs and new therapeutic agents and protocols on patient perspectives such as quality of life, adherence and satisfaction. The manuscript management system is completely online and includes a very quick and fair peer-review system, which is all easy to use. Visit http://www.dovepress.com/testimonials.php to read real quotes from published authors.

Submit your manuscript here: http://www.dovepress.com/immunotargets-and-therapy-journal